

# 3D KMC Reliability Simulation of Nano-Scaled HKMG nMOSFETs with Multiple Traps Coupling

Yun Li, Zhiyuan Lun, Peng Huang, Yijiao Wang, Hai Jiang, Gang Du\*, and Xiaoyan Liu\*

Institute of Microelectronics  
Peking University  
Beijing, 100871, China

\* Email: xyliu@ime.pku.edu.cn, gangdu@pku.edu.cn

**Abstract**—This paper presents coupling characteristics of multiple traps in HKMG nMOSFETs by a 3D kinetic Monte-Carlo (KMC) simulator we developed, which includes several fully-coupled multi-physical models: trap generation/recombination, trapping/detrapping to/from channel, metal gate, and the interaction of traps. It shows that activation energy and trapping/detrapping from/to channel/gate impact on coupling of multiple traps. Interaction of traps complicates mechanism in TAT current, BTI, and RTN.

**Keywords**—HKMG; nMOSFETs; 3D; kinetic Monte-Carlo; multiple traps; coupling; trap generation/recombination; capture time; emission time; threshold voltage shift; trapping; detrapping; PBTI;

## I. INTRODUCTION

Bias temperature instability (BTI), random telegraphy noise (RTN), and trap-assisted-tunneling (TAT) induced gate leakage current are major sources of reliability and variability concerns in nano-scaled high-K metal gate (HKMG) MOSFET [1,2]. They are mainly induced by defects trapping/detrapping [3,4]. Single trap analysis is relatively easy to achieve and understand, while multiple trap performance is complex due to the coupling behavior of traps. Moreover, because of the instability of HKMG process and material characteristics, different traps have different response to stress and temperature [5]. In addition, stress inducing new traps in high-K stack has been proved [3,6]. Regarding trapping/detrapping as the result of charging and discharging of oxygen vacancies in  $\text{HfO}_2$  is generally accepted [7,8]. Due to the complicated physical phenomenon, it is difficult to extract more detailed information only from measurements. Hence, comprehensive simulation of the traps system is quite necessary to further understand the behavior of multiple traps.

In this paper, a 3D KMC simulator is developed with consideration of coupling characteristics of multiple traps in HKMG nMOSFET. Simulated capture and emission time constants are compared with measurements. Transient characteristics of threshold voltage shift and traps interaction are investigated.

## II. SIMULATION METHOD

Fig. 1 shows the schematic of multi-physical models. Capture and emission time constant  $\tau_c$  and  $\tau_e$  are obtained by

multi-phonon model [9, 10]. Fig. 2 shows the simulation framework, in which probabilities of five processes are described by equation (1)-(10). It presents that trap generation/recombination, trapping/ detrapping to/from channel, metal gate, and the interaction of traps are fully-coupled.

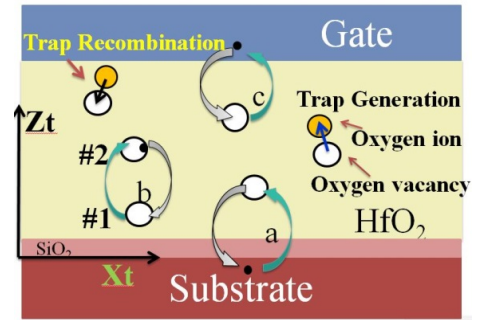


Fig. 1. Schematic of multi-physical models (a: trapping/detrapping from/to channel, b: trapping/detrapping from/to other traps, c: trapping/detrapping from/to channel).

Probabilities of trapping/detrapping are described by following equations:

a: Probability of trapping from Sub ( $k_c$ ) and detrapping to sub ( $k_e$ ).

$$k_c = \delta_{nc} v_n n \exp(\beta \epsilon_{12}) \quad (1)$$

$$k_e = \delta_{ne} v_n N_c \exp(\beta \epsilon_{21}) \quad (2)$$

b: Probability of trap i detrapping to trap j ( $k_{ij}$ ) and trapping from trap j ( $k_{ji}$ ).

$$k_{ij} = T_{ij} f_c \exp(\beta \epsilon_{ij}) \quad (3)$$

$$k_{ji} = T_{ji} f_e \exp(\beta \epsilon_{ji}) \quad (4)$$

c: Probability of trapping from gate ( $k_{cm}$ ) and detrapping to gate ( $k_{em}$ ).

$$k_{cm} = \delta_{nc} v_n n \exp(\beta \epsilon'_{12}) \exp(\alpha x) \quad (5)$$

$$k_{em} = \delta_{ne} v_n N_c \exp(\beta \epsilon'_{21}) \exp(\alpha x) \quad (6)$$

$$\epsilon_{12} = uc - \lambda (F/F_0)^p \quad (7)$$

$$\epsilon_{21} = ue + \lambda (F/F_0)^p \quad (8)$$

$v_n$  is thermal velocity ( $v_n = \sqrt{8k_B T / \pi m_n}$ ),  $m_n$  is tunneling mass,  $\delta_{nc}$ ,  $\delta_{ne}$  ( $\delta_{nc,e} = \delta_0 T_n$ ) are capture cross section times.  $T$  is temperature.  $f_c$ , and  $f_e$  are the attempt frequencies.  $\beta = 1/k_B T$ .  $k_B T$  is the thermal energy;  $\lambda$  and  $\rho$  are the enhancement factors of the electric field  $F$ ,  $uc$  and  $ue$  are active energies.  $T_{ij}$ ,  $T_{ji}$ , and  $T_n$  are the tunneling probabilities,  $n$  is the electron density.  $\mathcal{E}'_{12}$ ,  $\mathcal{E}'_{21}$ ,  $\mathcal{E}_{ij}$  and  $\mathcal{E}_{ji}$  are active energies calculated according to nonradiative multiphonon transition models [9].

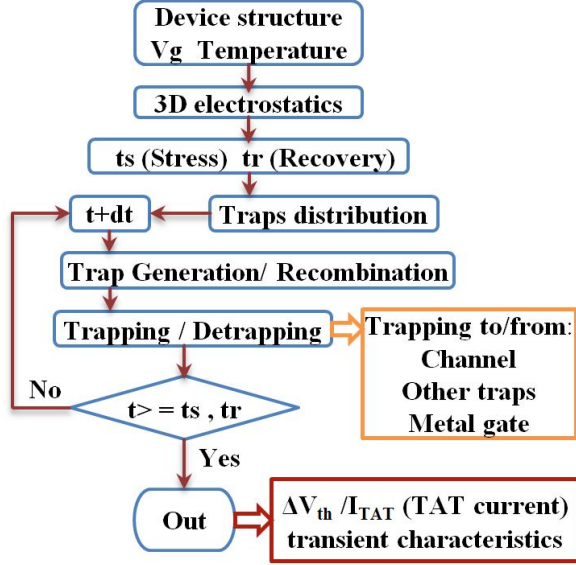


Fig. 2. 3D KMC simulation flowchart.

TABLE I. PARAMETERS IN SIMULATION

Para.	Values	Para.	Values
$f_g$	$5 \times 10^{11}$ Hz	$u_{c0}$	0.75 eV
$f_r$	$2 \times 10^{12}$ Hz	$u_{e0}$	0.45 eV
$f_{c,e}$	$2 \times 10^{13}$ Hz	$\sigma_c$	0.16 eV
$\lambda$	0.2eV	$\sigma_e$	0.1 eV
$F_0$	$10^2$ V/cm	$\rho$	1.5
$\gamma$	0.5 nm	$\alpha$	$10^7$ /cm
$m_n$	0.18	$\sigma_{Ea}, \sigma_{Er}$	0.2
$\mathcal{E}_{HfO2}$	22	$\delta_0$	$1 \times 10^{-14}$ cm <sup>2</sup>
$E_{a0}$	1.9eV	$u_c, u_e$	$N(u_{c0,e0}, \sigma_{c,e})$
$E_{r0}$	1.2eV	$E_a, E_r$	$N(E_{a0,r0}, \sigma_{Ea,Er})$

$N(u_0, \sigma)$  is Gaussian distribution.  $u_0$  is mean value.  $\sigma$  is mean-square deviation.

Trap generation probability is given by equation (9) [7], where  $E_a$  is the active energy modulated by electrical field. Furthermore, the new instable traps are likely recombination. Probability of trap recombination is determined by active energy  $E_r$  and temperature, as shown in equation (10) [11].

e: Probability of trap generation

$$P_g = f_g \exp(\beta(E_a - \gamma F)) \quad (9)$$

f: Probability of trap recombination

$$P_r = f_r \exp(\beta E_r) \quad (10)$$

$f_g, f_r$  are the attempt frequencies and  $\gamma$  is the enhancement factor of the electric field  $F$ . Threshold voltage shift  $\Delta V_{th}$  at time  $t+dt$  is obtained by considering the spatial contribution of occupied traps, including pre-existing and new ones. The occupation states of traps are caused by trapping/detrapping from/to substrate/gate/other traps during  $t$  to  $t+dt$ .

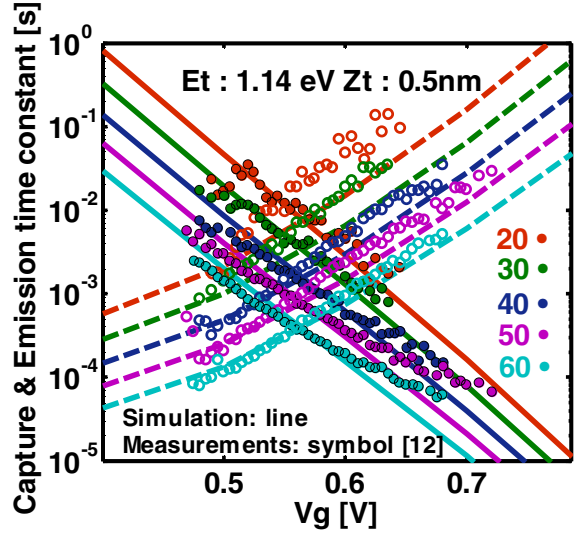


Fig. 3. Single trap  $\tau_c$  (solid symbol) and  $\tau_e$  (opened symbol) dependence on gate voltage  $V_g$  and temperature

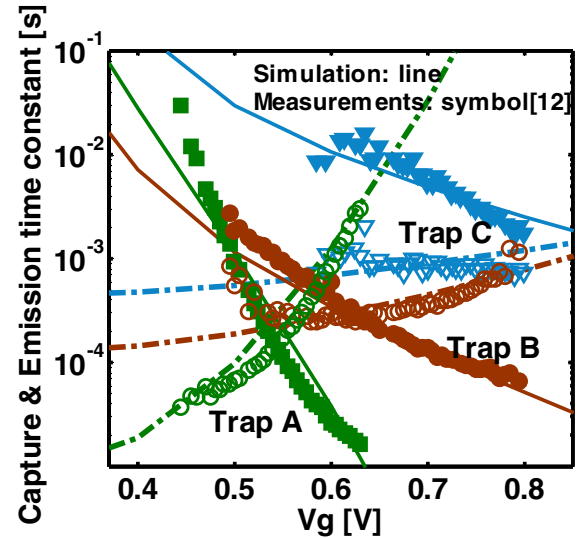


Fig. 4. Three traps  $\tau_c$  (solid symbol) and  $\tau_e$  (opened symbol) dependence on gate voltage  $V_g$  (Trap A:  $E_t$ : 0.904eV  $Z_t$ : 0.25nm; Trap B  $E_t$ : 1.185eV  $Z_t$ : 0.5nm; Trap C  $E_t$ : 1.156eV  $Z_t$ : 0.75nm).

Fig. 3 shows the simulated capture and emission time constants ( $\tau_c$  and  $\tau_e$ ) under different temperature, the measurement results in [12] are also plotted, in which  $\tau_e$  decreases with gate voltage  $V_g$  while  $\tau_c$  increases, indicating that the increase in temperature accelerates trapping/detrapping process. It can be seen that well agreement between the simulation results and the measurement data.

Fig. 4 shows the  $\tau_c$  and  $\tau_e$  of three independent traps as functions of  $V_g$ , which is in good agreement with experimental data [12]. Simulation results in Fig. 4 indicate differences in location and energy level  $E_t$  between trap A, B and C. The parameters used in the simulator are listed in Table I.

### III. RESULTS AND DISCUSSION

In order to investigate the coupling of multiple traps, a 5nm HfO<sub>2</sub> stack with two traps is simulated, as shown in Fig. 1. Fig. 5 shows the ratio of  $\Delta V_{th}$  to maximum  $\Delta V_{th}$  in a two-trap system. It can be observed in Fig. 5 that charge exchange between the traps can cause fluctuations in transient waveform of threshold voltage shift. Fig. 6 shows the  $\Delta V_{th}$  transient characteristics under different capture and emission activation energy (uc and ue) of two traps. It can be seen that  $\tau_c$  increases with larger activation energy of the capture event and  $\tau_e$  increases with larger activation energy of emission event. The states of trap #1, #2 are impacted by capture/emission charge from/to channel and each other, simultaneously.

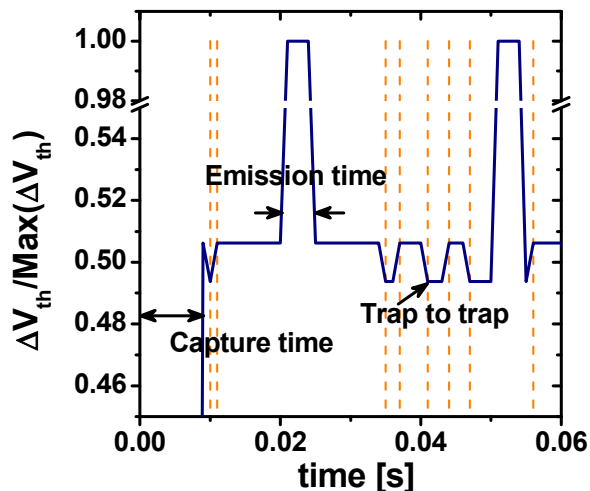


Fig. 5. Trap-to-trap tunneling occur at shallow vertical line

Fig. 7 shows the dependence of trap-to-trap time constant  $\tau_{tt}$  on the emission (ue) and capture (uc) active energy. It can be seen that trap-to-trap time constant  $\tau_{tt}$  (#1 detrapping to #2 or #2 detrapping to #1) increases with larger activation energy of  $\tau_c$  and  $\tau_e$ . The time constant of #2 detrapping to #1 is larger than the time constant of #1 detrapping to #2. However, statistical  $\tau_{tt}$  (average time of exchanging charge) extracted from  $\Delta V_{th}$  transient characteristics in Fig. 6 decreases at first and then increases from  $ue=0.74\text{eV}$  and  $uc=0.43\text{eV}$  respectively. It indicates that when ue is large enough, the charged traps cannot capture other electrons, while when ue is

too small, small charge occupancy rate cannot enable the trap-to-trap tunneling. Similarly, smaller uc results in charged traps while larger uc is related to lower probability of trapping event. It reveals that multiple trap coupling is a compound process with trapping/detrapping from/to gate/channel rather than simple independent event.

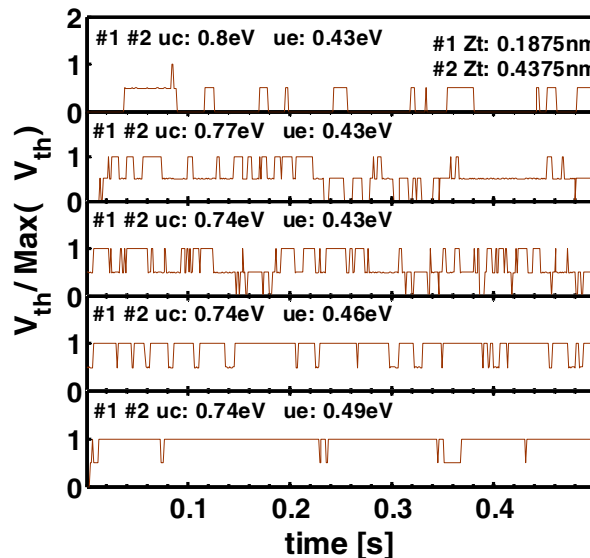


Fig. 6.  $\Delta V_{th}$  transient characteristic with different uc, ue ( $V_g=0.6\text{V}$   $T=300\text{k}$ , include 2 coupling traps)

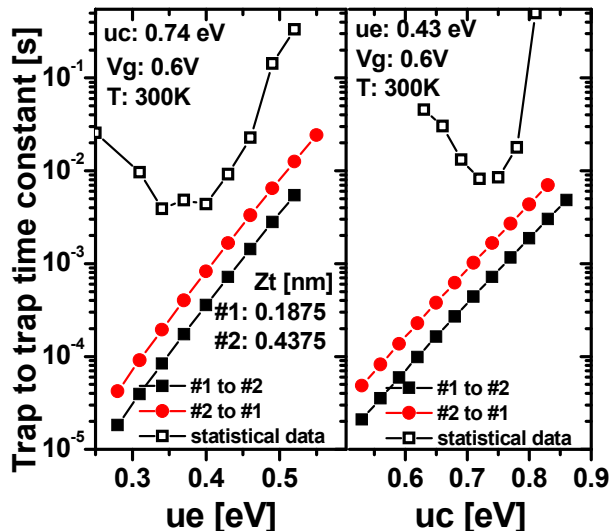


Fig. 7.  $\tau_{tt}$  dependence on emission (ue) and capture (uc) active energy

Fig. 8 shows the dependence of trap-to-trap time constant  $\tau_{tt}$  on distance along  $Z_t$ . It can be seen that  $\tau_{tt}$  increases exponentially with growing distance along oxide thickness  $Z_t$  and the tunneling probability increases with larger  $\Delta Z_t$  (the distance between trap #1 and #2).  $\tau_{tt}$  of trap #1 to #2 increases more slowly with  $\Delta Z_t$  than  $\tau_{tt}$  of trap #2 to #1, while  $\tau_{tt}$  of trap #2 to #1 have same rate of increase as statistical results.

Fig.9 shows the PBTI phenomenon of nMOSFET induced by the charging events of five traps located at fixed position with Gaussian energy distribution. It indicates that traps with different activation energy result in an obvious difference in threshold voltage shifts. Trapping/Detrapping from/to other traps provide more possibilities of threshold voltage shifts and increase the complexity of analysis.

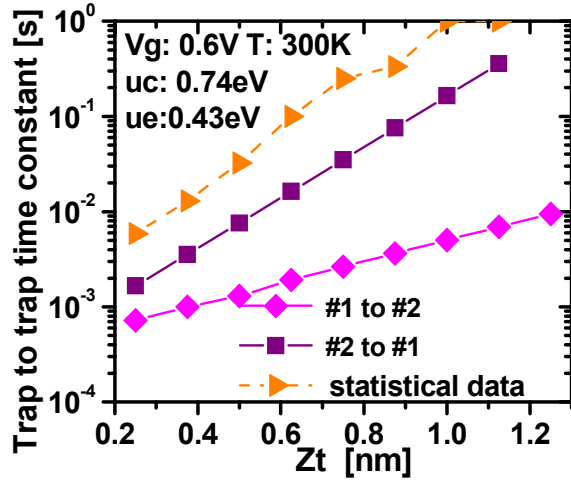


Fig. 8. Trap-to-trap time constant  $\tau_t$  dependence on distance along  $Z_t$ .

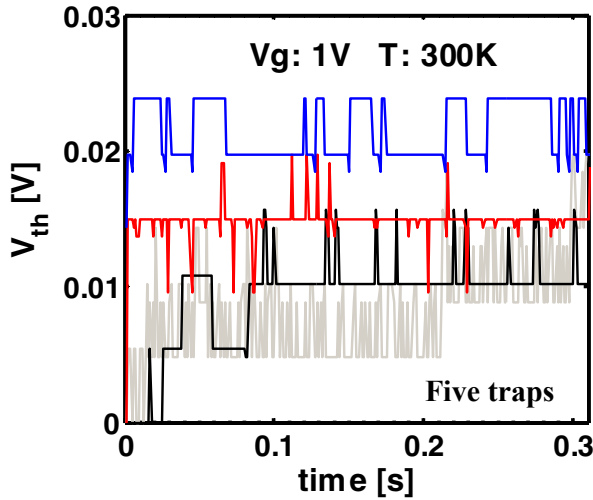


Fig. 9. PBTI induced by trapping (Different colors are related different Gaussian energy distributions.  $\sigma=0.16$  eV  $\sigma=0.1$  eV).

#### IV. SUMMARY

We have modeled the coupling effects of multiple traps and developed a 3D KMC simulator to investigate the multiple traps interaction behaviors. The results indicate that the

interaction of multiple traps is much more complex than single trap, which aggravates reliability and variability analysis, induces new mechanism in TAT current, BTI, and RTN. Traps coupling can induce distraction of time constant extraction in measurement especially in material with high trap density.

#### ACKNOWLEDGMENT

This work is supported by the National Fundamental Basic Research Program of China Grant No 2011CBA00600 and NSFC Grant No. 61250014.

#### REFERENCES

- [1] A. Kerber, T. Nigam, "Challenges in the characterization and modeling of BTI induced variability in Metal Gate / High-k CMOS technologies," IRPS, pp. 2D.4.1 - 2D.4.6, 2013.
- [2] S. Cimino, A. Padovani, L. Larcher, V.V. Afanas'ev, H.J. Hwang, Y.G. Lee, M. Jurczak, D. Wouters, B.H. Lee, H. Hwang, L. Pantisanoa "A study of the leakage current in TiN/HfO<sub>2</sub>/TiN capacitors," Microelectronic Engineering 95, pp. 71-73, 2012.
- [3] E. R. Hsieh, P. Y. Lu, Steve S. Chung, K. Y. Chang, C. H. Liu, J. C. Ke, C. W. Yang, and C. T. Tsai, "The Experimental Demonstration of the BTI-Induced Breakdown Path in 28nm High-k Metal Gate Technology CMOS Devices," VLSI Technology, pp. 132-133, 2014.
- [4] Maria Toledano-Luque, Robin Degraeve, Philippe J. Roussel, Lars-Åke Ragnarsson, Thomas Chiarella, Naoto Horiguchi, Anda Mocuta, and Aaron Thean, "Fast Ramped Voltage Characterization of Single Trap Bias and Temperature Impact on Time-Dependent VTH Variability," IEEE TED vol. 61, pp. 3139-3144, September 2014.
- [5] C. M. Chang, Steve S. Chung, Y. S. Hsieh, L. W. Cheng, C. T. Tsai, G. H. Ma, S. C. Chien, and S. W. Sun, "The Observation of Trapping and Detrapping Effects in High-k Gate Dielectric MOSFETs by a New Gate Current Random Telegraph Noise (IG-RTN) Approach," IEDM, pp. 1-4, 2008.
- [6] D. P. Ioannou, "HKMG CMOS technology qualification: The PBTI reliability challenge," Microelectronics Reliability, pp. 1489-1499, 2014.
- [7] Y. J. Wang, P. Huang, X. Y. Liu, G. Du, J. F. Kang, "Time Dependent 3-D Statistical KMC Simulation of High-k Degradation Including Trap Generation and Electron Capture/Emission Dynamic," SISPAD, pp. 85-88, 2014.
- [8] K. Zhao, J. H. Stathis, B. P. Linder and E. Cartier, A. Kerber, "PBTI under dynamic stress: from a single defect point of view," IRPS, pp. 4A.3.1-4A.3.9, 2011.
- [9] T. Grasser, "Stochastic charge trapping in oxides: From random telegraph noise to bias temperature instabilities," Microelectronics Reliability, pp. 39-70, November, 2012.
- [10] F. Schanovsky, O. Baumgartner and T. Grasser, "Multi Scale Modeling of Multi Phonon Hole Capture in the Context of NBTI," SISPAD, pp. 15-18, 2011.
- [11] X. M. Guan, S. M. Yu, and H.-S. Philip Wong, "On the Switching Parameter Variation of Metal-Oxide RRAM—Part I: Physical Modeling and Simulation Methodology," IEEE TED 2012, vol. 59, no. 4, pp. 1172-1182
- [12] H. Miki, N. Tega, M. Yamaoka, D. J. Frank, A. Bansal, M. Kobayashi, K. Cheng, C. P. D'Emic, Z. Ren, S. Wu, J-B. Yau, Y. Zhu, M. A. Guillorn, D-G. Park, W. Haensch, E. Leobandung, and K. Torii, "Statistical Measurement of Random Telegraph Noise and Its Impact in Scaled-down High- k/Metal-gate MOSFETs," IEDM, pp. 450-453, 2012.